Metabolism of Lipid Derived Aldehyde, 4-Hydroxynonenal in Human Lens Epithelial Cells and Rat Lens

Sanjeev Choudhary,[1] *Sanjay Srivastava,*[2] *Tianlin Xiao,*[1] *Usha P. Andley,*[3] *Satish K. Srivastava,*[1] *and Naseem H. Ansari*[1]

Purpose. An earlier study showed that 4-hydroxynonenal (HNE), formed as a result of increased lipid peroxidation in oxidative stress, causes loss of lens transparency. To determine how HNE is detoxified in ocular tissues, its metabolism in cultured human lens epithelial cells (HLECs) as well as rat lens was investigated.

Methods. Rat lens or HLECs were incubated with 30 nmol (5×10^5 cpm/μmol) of HNE in 2 mL Krebs-Hansleit buffer for 1 hour at 37°C. The medium, after ultrafiltration was analyzed by high performance liquid chromatography (HPLC), using a C-18 reversed-phase column. The metabolites were separated by using a gradient consisting of solvent A (0.1% aqueous trifluoroacetic acid) and solvent B (100% acetonitrile) at a flow rate of 1 mL/min. Fractions containing radioactivity were pooled and analyzed using electrospray ionization mass spectroscopy (ESI-MS) or gas chromatography–chemical ionization mass spectroscopy (GC/CI-MS).

Results. On HPLC, the incubation media from cultured lens and HLECs separated into three major radioactive peaks. Peak I of the HLECs and lens treated with HNE was identified to be a mixture of glutathione (GS) conjugates of HNE and 1,4-dihydroxy-2-nonene (DHN). The identity of the conjugates was confirmed by ESI-MS. Based on the retention times, peaks II, and III were assigned to 4-hydroxy-2-nonenoic acid (HNA) and unmetabolized HNE, respectively. The identities of HNA and HNE were confirmed by spiking the tissue extracts with synthetic metabolites and finally by GC/CI-MS. Sorbinil, an aldose reductase (AR) inhibitor, attenuated GS-DHN levels and cyanamide, an aldehyde dehydrogenase inhibitor, decreased formation of HNA.

Conclusions. The results show that the major metabolic transformation of HNE in rat lens and HLECs involves conjugation with GS and oxidation to HNA. The GS-HNE conjugate is reduced to GS-DHN by AR. Thus, under normal physiological conditions, the lens has multiple routes to detoxify HNE. However, oxidative stress may overwhelm the metabolic capacity of the lens to detoxify HNE and lead to formation of cataract. (*Invest Ophthalmol Vis Sci.* 2003;44:2675–2682) DOI:10.1167/iovs.02-0965

Cellular damage, caused by the reactive oxygen species, occurs in the biological system because of an inadequate detoxification of free radicals that results in the accumulation of chemically altered macromolecules. Proteins, nucleic acids, and particularly the polyunsaturated fatty acids, that constitute the biological membranes, are vulnerable to oxidation by free radicals. Lipid peroxides thus formed are degraded to lipid-derived aldehydes (LDAs), which are believed to contribute to the pathogenesis of several diseases such as diabetes, aging, retinopathy of prematurity, ischemia, and cancer.[1–3] LDAs, are more stable than their precursor free radicals and thus can diffuse from the initial site of lipid peroxidation and propagate oxidative injury by acting as s toxic messenger. LDAs such as malonaldehyde (MDA), acrolein, and 4-hydroxynonenal (HNE) have received special attention in the development of oxidative diseases. Of the various LDAs, HNE and 4-hydroxyhexenal (HHE), arising from the peroxidation of arachidonic acid and docosahexaenoic acid, respectively, are the most toxic and are generated in high concentrations.[4] Because these aldehydes are electrophilic in nature, they readily react with nucleophiles, such as thiols and amines, and exert marked biological effects that, depending on their concentration, can cause selective alterations in cell signaling, protein and DNA damage, and cytotoxicity.[2,5]

The ocular lens is a potential target of reactive oxygen species, generated as the by-products of cellular metabolism or the result of photochemical reactions. Constant exposure to high levels of irradiation provides an ideal environment for the generation of reactive oxygen species in the ocular tissues.[6,7] Existence of various metabolic pathways and metabolites of arachidonic acid in the lens[8–10] indicates the presence of polyunsaturated fatty acids (PUFAs) in this tissue. Although it is known that the ocular lens (whole) has low levels of unsaturated lipids,[11] the distribution of unsaturated lipids is not uniform throughout the lens.[12,13] The propensity of unsaturation is more in the exterior region compared with the interior region of the lens. We have also observed (Kaphalia BS, Xiao TL, Ansari GAS, Ansari NH, unpublished data, 2003) that the lens epithelium in various species has at least 15 to 20 times more unsaturated lipids per milligram protein than does the cortex and nucleus. We have reported that human lens epithelial cells exposed to oxidative stress generate high levels of HNE.[14] Lipid peroxidation products, such as, HNE, can form protein-HNE adducts that may result in altered protein functions. We have also shown the presence of elevated levels of protein–HNE adducts in human diabetic lenses using the antibodies against Michael adducts of protein–HNE (Ansari NH, Khanna P, Bhatnagar A, Bhalla P, Szweda L, ARVO Abstract 5452, 1997). Some LDAs that are found in the lens may be generated in the retina. It has been suggested that degenera-

From the [1]Department of Human Biological Chemistry and Genetics, University of Texas Medical Branch, Galveston, Texas; the [2]Department of Medicine, Division of Cardiology, University of Louisville, Kentucky; [3]Department of Ophthalmology, Washington University School of Medicine, St. Louis, Missouri.

Supported in part by NIH Grants EY13014 (NHA), HL61618 (SS), EY01677 (SKS), and EY05681 (UPA); and the Lions Eye Bank Foundation (NHA).

Submitted for publication September 19, 2002; revised November 22, 2002; accepted January 13, 2003.

Disclosure: **S. Choudhary**, None; **S. Srivastava**, None; **T. Xiao**, None; **U.P. Andley**, None; **S.K. Srivastava**, Pfizer (F); **N.H. Ansari**, None

The publication costs of this article were defrayed in part by page charge payment. This article must therefore be marked "*advertisement*" in accordance with 18 U.S.C. §1734 solely to indicate this fact.

Corresponding author: Naseem H. Ansari, Department of Human Biological Chemistry and Genetics, University of Texas Medical Branch, Galveston, TX 77555-0647; nansari@utmb.edu.

Copyright © Association for Research in Vision and Ophthalmology

Downloaded from iovs.arvojournals.org on 06/16/2019

tion of rod outer segments in retinal-degeneration diseases can produce LDAs such as MDA, which could be responsible for the lens clouding in such retinal diseases.[15–17] Nevertheless, regardless of the source of HNE, we have demonstrated that micromolar concentrations of HNE cause opacification of rat lens in culture[18] and that LDAs induce apoptosis in human lens epithelial cells (HLECs).[19] Because LDAs are toxic and can be generated in the lens, this tissue should have adequate mechanism to detoxify such aldehydes. The metabolism of LDAs has been extensively investigated, mainly in nonocular tissues such as liver, heart, and erythrocytes.[20–22] In nonocular tissues, three main enzymatic routes of HNE detoxification (see Scheme 1) have been identified: (1) enzymatic conjugation of HNE with glutathione (GS) catalyzed by glutathione *S*-transferases or nonenzymatic conjugation to form GS-HNE; (2) reduction of HNE and GS-HNE by aldo- and ketoreductases and alcohol dehydrogenase leading to the formation of (1,4-dihydroxy-2-nonene) DHN and GS-DHN, respectively; and (3) oxidation of HNE to 4-hydroxy-2-nonenoic acid (HNA) by aldehyde dehydrogenase and carbonyl reductases.[2] Because the reactive LDAs, such as HNE, are continuously generated in ocular tissues and their metabolic fate is unknown, in the present study we systematically examined the contribution of various metabolic pathways to the detoxification of HNE in the ocular lens and HLECs.

Materials and Methods

Materials

Aldehyde dehydrogenase, cyanamide, reduced glutathione (GSH), fetal bovine serum (FBS), and trypsin were purchased from Sigma Chemical Co. (St. Louis, MO). Trifluoroacetic acid (TFA) was obtained from Pierce (Rockford, IL). Dulbecco's minimum essential medium (DMEM) and phosphate-buffered saline (PBS) were purchased from Gibco Laboratories (Grand Island, NY). Sorbinil was a gift from Pfizer (Groton, CT). All other reagents were of the highest purity available. Male Sprague-Dawley rats in the weight range of 100 to 150 g (obtained from Harlan, Houston, TX) were killed on the day of the experiment by cervical dislocation. The optic globes were removed, and the lenses with intact capsules were carefully dissected. All investigations were performed according to the ARVO Statement for the Use of Animals in Ophthalmic and Vision Research. HLECs with extended life span (HLE-B3 cells), described previously,[23] were used in the study. Cells were grown in Eagle's MEM (Sigma) containing 50 μg/mL gentamicin and 20% FBS in an atmosphere of 5% CO_2 and air at 37°C. The pH of the medium was adjusted to 6.8 to 7.0, before sterile filtration and addition of serum. Cells were fed twice a week and after attaining confluence were passaged using trypsin-EDTA. The GSH content of these cells was 46.8 ± 2.66 nmol/mg protein and in the lens 5.13 ± 0.038 mM, as determined spectrophotometrically using 5,5′-dithiobis(2-nitrobenzoic acid).[24]

Chemical Synthesis

[4-^{3}H] HNE was synthesized as its dimethyl acetal as described by us earlier.[25] Before use, [4-^{3}H] HNE was obtained by acid hydrolysis of dimethyl acetal and purified by HPLC. The [4-^{3}H] HNE thus synthesized had a specific activity of approximately 90 mCi/mmol. Radiolabeled DHN was synthesized enzymatically by incubating 60 nmol of [4-^{3}H] HNE with 300 mU of human placental recombinant aldose reductase (AR) and 0.1 mM reduced nicotinamide adenine dinucleotide phosphate (NADPH) in 0.05 M potassium phosphate (pH 6.0) containing 0.4 M Li_2SO_4. The reaction was monitored by following the decrease in absorbance at 224 nm. At the end of the reaction, the enzyme was removed by ultrafiltration (Centriprep-10; Millipore, Bedford, MA) and DHN in the filtrate was purified by HPLC, as described later. Radiolabeled [4-^{3}H] HNA was synthesized by incubating 100 nmol of [4-^{3}H] HNE with 1.0 U of aldehyde dehydrogenase and 1.5 mM nicotinamide adenine dinucleotide (NAD) in 0.1 mM potassium phosphate (pH 7.4) at 25°C. The reaction was monitored by observing the increase in absorbance at 340 nm. The enzyme was removed by ultrafiltration and HNA in the filtrate was purified by HPLC. The identity and the purity of the HNE, DHN, and HNA were established by gas chromatography–chemical ionization mass spectroscopy (GC/CI-MS).

The conjugate of GSH and HNE was synthesized by incubating 0.5 μmol [4-^{3}H] HNE with 2 μmol of GSH and 0.1 M potassium phosphate (pH 7.0) in a 1 mL system, at 37°C. The conjugation was observed by monitoring the decrease in absorbance at 224 nm for 30 minutes. GS-HNE was purified by HPLC and characterized by electrospray-ionization mass spectroscopy (ESI-MS). GS-DHN was synthesized by the reduction of GS-HNE in the presence of 250 mU of recombinant AR and 0.1 mM potassium phosphate (pH 7.0) at 37°C. The reaction was observed by monitoring the decrease in absorbance at 340 nm for 30 minutes. The reaction mixture was ultrafiltered, and the filtrate was purified by HPLC and characterized by ESI-MS.

HPLC Analysis

Synthetic HNE and its possible metabolites were separated by HPLC with a reversed phase C-18 column (ODS; Varian Analytical Instruments, Walnut Creek, CA), pre-equilibrated with 0.1% aqueous trifluoroacetic acid (TFA) at a flow rate of 1 mL/min. The compounds were eluted with a gradient consisting of solvent A (0.1% aqueous TFA) and solvent B (100% acetonitrile) at a flow rate of 1 mL/min. The gradient was established either as described earlier[22] or so that solvent B reached 17% in 10 minutes and was held at this level for 60 minutes. In the next 5 minutes, solvent B reached 50% and in an additional 5 minutes, 100%. Fractions (1 mL) were collected and the radioactivity in each fraction was measured in a 100-μL aliquot with a liquid scintillation counter (Beckman Instruments, Fullerton, CA).

Electrospray Ionization Mass Spectrometry

For the characterization of the GS conjugates, ESI mass spectra were acquired on a single-quadrapole instrument (LCZ; Micromass, Manchester, UK). The ESI-MS operating conditions were as follows: capillary voltage, 3.0 kV; cone voltage, 25 V; extractor voltage, 4 V; source block temperature, 80°C; and dissolvation temperature, 200°C. Nitrogen at 3 psi was used as nebulizer gas. Samples were reconstituted in 100 μL acetonitrile-water-acetic acid 50:50:0.1 (vol/vol/vol) and then injected into the mass spectrometer with a syringe pump (Harvard Apparatus, Holliston, MA) at a rate of 10 μL/minutes. Spectra were acquired at the rate of 200 atomic mass units/second over the range of 100 to 650 atomic mass units.

Gas Chromatography–Chemical Ionization Mass Spectrospray

For GC/CI-MS analyses of DHN, HNA, and HNE, the samples were derivatized in 20 μL of acetonitrile with 20 μL *N,O*-bis(trimethylsilyl)-trifluoroacetamide (BSTFA) for 1 hour at 60°C. The mixture was cooled to room temperature, and 1-μL aliquots were used for analysis. The GC/CI-MS analysis was performed (model HP5890/HP5973 GC/CI-MS system; Hewlett Packard, Palo Alto, CA) under 70 eV electron ionization conditions. The compounds were separated on a bonded phase capillary column (DB-5MS, 30 m × 0.25 mm internal diameter × 0.25-μm film thickness; J7W Scientific, Folsom, CA). The GC injection port and interface temperatures were set to 280°C, with helium gas (carrier) maintained at 14 psi. Injections were made in the splitless mode with the inlet port purged for 1 minute after injection. The GC oven temperature was held initially at 100°C for 1 minute, then increased at a rate of 10°C/minute to 280°C, which was held for 5 minutes. Under these conditions, the retention time (τ_R) for the HNA derivative was 9.94 minutes.

Metabolic Studies

The rate of HNE consumption by the rat lens and HLECS was investigated first to determine the appropriate time of incubation of these tissues for metabolic studies.

Downloaded from iovs.arvojournals.org on 06/16/2019

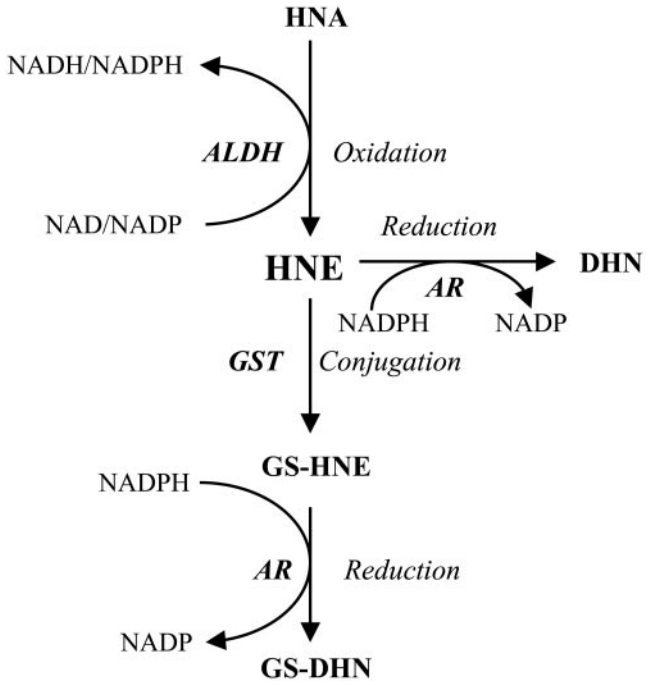

SCHEME 1. Metabolic pathways of HNE.

Freshly isolated rat lenses, free of connective tissue, were washed twice with PBS and individually incubated with 30 nmol (15,000 cpm) [4-^{3}H] HNE at 37°C in an atmosphere of 5% CO_2 in air for 0 to 90 minutes in 2.0 mL of Krebs-Hansleit (K-H) buffer (concentration in mM: NaCl 118, KCl 4.7, $MgCl_2$ 1.25, $CaCl_2$ 30, KH_2PO_4 1.25, EDTA 0.5, NaH CO_3 25, and glucose 10 [pH 7.4]). Under these incubation conditions, no change in the pH of the medium was observed during the course of the experiments. At each time point, 100 μL of the incubation medium was withdrawn and ultrafiltered (Centriprep-10; Millipore). The filtrate thus obtained was applied to a C-18 reversed-phase HPLC column (ODS; Varian), and unmetabolized HNE was quantified by determining the radioactivity in the fractions corresponding to the τ_R of standard HNE.

HLECs (0.8×10^6) were washed twice with PBS and incubated with 30 nmol (15,000 cpm) [4-^{3}H] HNE in 2.0 mL K-H buffer in an atmosphere of 5% CO_2 in air for 0 to 60 minutes. Under these incubation conditions, no change in the pH of the medium was observed during the course of the experiment. At each time point, 100-μL aliquots of the incubation medium were withdrawn and processed to measure the unmetabolized HNE.

Rat lens or 0.8×10^6 HLECs were preincubated with 50 μM sorbinil or 2.0 mM cyanamide for 30 minutes in 2.0 mL K-H buffer followed by incubation with 30 nmol [4-^{3}H] HNE for 60 and 30 minutes, respectively, at 37°C, with continuous shaking. At the end of incubation, the incubation media was ultrafiltered, and the metabolites were resolved by HPLC and analyzed as described earlier.

RESULTS

HNE Consumption

When rat lenses were incubated with 30 nmol [4-^{3}H]HNE, approximately 50%, 60%, and 70% was consumed in the incubation medium in 30, 60, and 90 minutes, respectively (Fig. 1A), as determined by the ^{3}H HNE remaining in the incubation medium. The rate of HNE consumption in the HLECs was relatively higher compared with that in the lens. Approximately 50% of the HNE was consumed in 10 minutes and in 60 minutes of incubation, approximately 90% of the HNE was consumed (Fig. 1B).

HNE Metabolism

Figure 2A shows the separation of the synthetic HNE metabolites on HPLC. In this system, the GS conjugates (GS-HNE and GS-DHN) eluted with a τ_R of 24 minutes, whereas DHN, HNA, and HNE eluted at a τ_R of 43, 54, and 67 minutes, respectively. The GS conjugates were characterized by ESI-MS and DHN, HNA, and HNE by GC/CI-MS. Three to four peaks were obtained on HPLC separation of the incubation medium of the lens or HLECs incubated with ^{3}H-HNE for 60 and 30 minutes, respectively (Figs. 2B, 2C). The peaks were tentatively assigned to HNE metabolites on the basis of the τ_R of the synthesized standards. To confirm the identity of various metabolites, the peak samples were individually spiked with known amounts of synthetic radiolabeled HNE and its putative metabolites. The coelution of synthetic metabolites with the putative assigned peaks confirmed our assignments. Because we did not observe any cross-contamination of metabolites in different peaks except peak I, which was found to be a mixture of GS-HNE and GS-DHN, all the values shown in Table 1 were calculated based

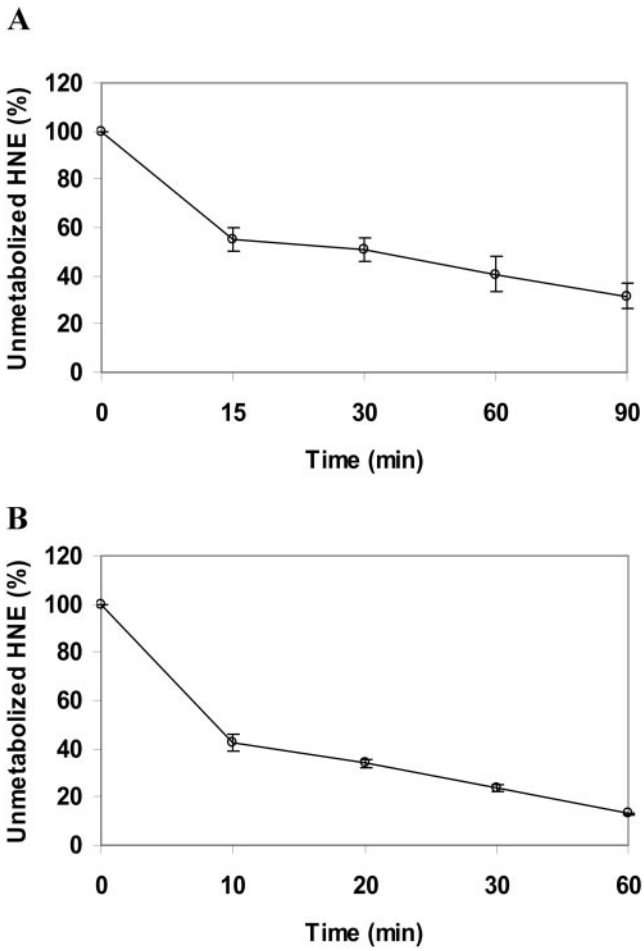

FIGURE 1. HNE consumption in the rat lens (**A**) and HLECs (**B**). Rat lens and HLECs (0.8×10^6) were incubated with 30 nmol [4-^{3}H] HNE for the indicated times, and the metabolites present in the incubation medium were resolved by HPLC. The percentage of HNE remaining in the medium was plotted as a function of time and expressed as the mean ± SD. No spontaneous disappearance of HNE was observed in the control incubation medium without the rat lens or HLECs (data not shown).

Downloaded from iovs.arvojournals.org on 06/16/2019

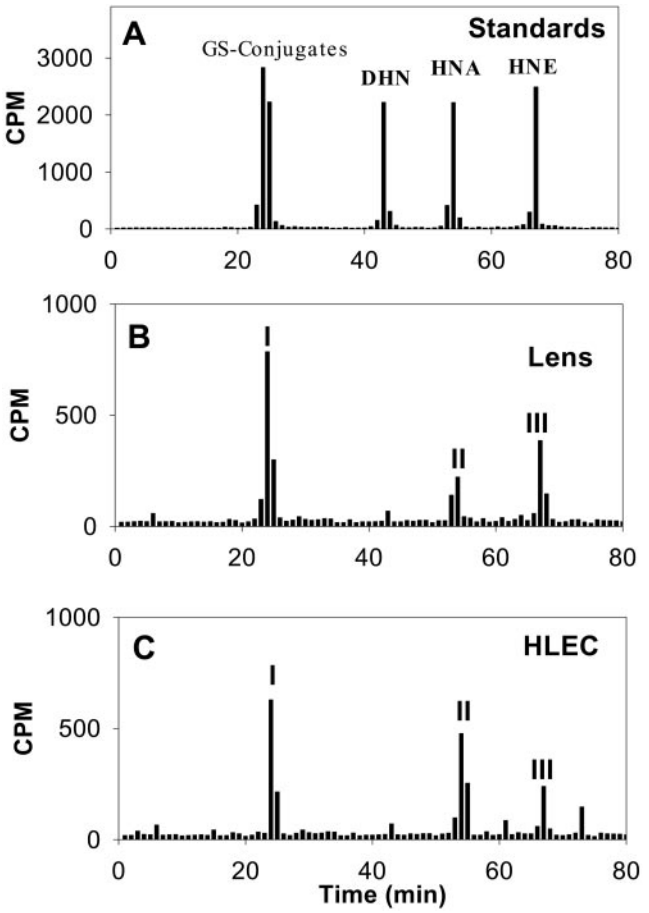

FIGURE 2. HNE metabolism in rat lens and HLECs. (**A**) HPLC profile of synthesized putative metabolites of [4-^{3}H] HNE. Tritiated HNE, DHN, GS-HNE, and GS-DHN were synthesized. Individually and in a mixture, they were resolved by reversed-phase HPLC. Only the elution profile of the mixture is given. GS conjugates (GS-HNE and GS-DHN) eluted with a τ_R of 24 minutes, whereas DHN, HNA, and HNE were eluted with a τ_R of 43, 54, and 67 minutes, respectively. (**B**) Typical HPLC profile of radiolabeled metabolites of HNE in the incubation medium of rat lens incubated with [4-^{3}H] HNE. Peak I corresponds to the synthetic GS conjugates of HNE and DHN, peak II to HNA, and peak III to unmetabolized HNE. (**C**) HPLC profile of radiolabeled metabolites of HNE in the medium of HLECs incubated with [4-^{3}H] HNE. Peaks I, II, and III correspond, respectively, to the GS conjugates of HNE and DHN, HNA, and unmetabolized HNE. An additional peak was observed with a τ_R of 73 minutes but was not characterized. In all the cases, peak I was characterized by ESI-MS and peaks II and III by GC/CI-MS.

on the radioactivity determination in each peak. The relative abundance of GS-HNE and GS-DHN in peak I was determined by ESI-MS. The peak with τ_R of 73 minutes and a minor peak at 61 minutes, observed only in HLECs, were not characterized. Similarly, in both the lens and HLECs an extremely minor peak eluted at 43 minutes, corresponding to DHN, was insufficient for further characterization.

ESI-MS of the synthetic GS-HNE showed a pseudomolecular ion $[MH]^+$ with a mass-to-charge ratio (m/z) of 464.2 (Fig. 3A). An additional species with m/z of 446.2 was also observed, which completely disappeared by decreasing the cone voltage and temperature with a concomitant increase in the 464.2 species, indicating that 446.2 species is the daughter ion formed by the dehydration of the 464.2 species. However, low cone voltage and temperature were also associated with eightfold decrease in the signal intensities, and therefore, these tune conditions were not used to analyze the conjugate in the incubation medium of the experimental samples. ESI-MS of the synthesized GS-DHN conjugate showed a single pseudomolecular ion $[MH]^+$ with an m/z of 466.2 and did not fragment under our experimental conditions (Fig. 3B). To calculate the relative proportion of GS-HNE and GS-DHN in the samples, we used the ratio of m/z (464.2 + 446.2) to 466.3. The arbitrary counts of these ions are given in Figure 3 along with the peaks. Peak I of the incubation medium of the lens/HLECs incubated with ^{3}H-HNE was identified to be glutathionyl conjugates of HNE. Fractions under peak 1 were pooled, lyophilized, and reconstituted in acetonitrile-water-acetic acid 50:50:0.1% (vol/vol/vol) and resolved by ESI-MS. When rat lens was incubated with 30 nmol of HNE, ESI-MS of peak I showed a predominant ion with m/z 446.2 which represents the daughter ion of GS-HNE. Signal at m/z 466.2 showed the formation of GS-DHN. The relative abundance of GS-HNE to GS-DHN was 2.5:1 (Fig. 3C) indicating that the extruded conjugate in rat lens was predominantly GS-HNE. ESI-MS of peak I obtained from HNE metabolism in HLECs showed a predominant ion with m/z 466.2, which was assigned to the +1 charge state of GS-DHN. The ion with m/z 464.2 which corresponds to the +1 charge state of GS-HNE was found to be negligible in amount, whereas the dehydrated species of GS-HNE with m/z 446.2 represented 25% of the GS-DHN signal (Fig. 3E). The distribution of the molecular ions show the relative abundance of GS-HNE and GS-DHN to be 1:4 indicating that the extruded GS conjugate of HNE in HLECs is predominantly in the reduced form. The peak at 448.2 in the HLECs appears to have come from the background, because an identical peak was observed in the HPLC fractions corresponding to the glutathionyl conjugates in the HLECs incubated in the absence of HNE (Fig. 3E, inset).

Figure 4A shows the gas chromatography (GC) chromatogram of reagent HNA (τ_R 9.94 minutes). Peaks at 14.17 and 21.3 minutes were from the derivitizing reagents or running solvents. Figure 4B shows the GC elution profile of peak II (τ_R of 54 minutes), obtained on HPLC of the incubation medium of the HLECs in Figure 2C, tentatively assigned to be HNA (based on the τ_R and spiking the peak with synthetic HNA). The peak was derivatized with BSTFA and resolved by GC/CI-MS. Similar to the reagent HNA, a prominent peak was observed at 9.94 minutes. The fragmentation pattern of the species eluted at 9.94 minutes showed fragments at m/z 73, 83, 147, and 245 (Figs. 4C, 4D), similar to those of synthetic HNA described by us earlier.[21,22] Peak II (τ_R of 54 minutes), shown in Figure 2B, obtained on HPLC of the incubation medium of the lens was similarly characterized to be HNA. HNA accounted for only 11% of total HNE metabolites in the rat lens, whereas in HLECs it corresponded to 28% (Table 1). The HPLC profiles of the incubation mixture of the lens and HLECs did not show any detectable peak close to 43 minutes, the τ_R of synthetic DHN.

Metabolic Pathways

As shown by the HPLC profile and Table 1, the major routes of HNE metabolism in the rat lens and the HLECs appear to be conjugation with GSH to form GS-HNE, which is subsequently reduced to GS-DHN and oxidation of HNE to HNA. To identify the biochemical pathways involved in the generation of these metabolites, rat lens or HLECs were preincubated either with or without inhibitors of AR (50 μM sorbinil) or aldehyde dehydrogenase (2 mM cyanamide) in 2.0 mL of K-H buffer at 37°C for 30 minutes. Subsequently, the lenses were incubated for 60 minutes and the HLECs for 30 minutes with [4-^{3}H] HNE.

When the lens was incubated with 30 nmol [4-^{3}H] HNE, approximately 65% of the HNE added was conjugated with GSH. In the presence of sorbinil, the relative abundance of GS-HNE:GS-DHN was 10:1 (Fig. 3D) as opposed to 2.5:1 in the absence of sorbinil (Fig. 3C), indicating that the extruded

Downloaded from iovs.arvojournals.org on 06/16/2019

TABLE 1. Metabolites of [^{3}H] HNE Recovered on HPLC Separation of the Medium of the Lens and HLECs Incubated with 30 nmol [4-^{3}H] HNE

Sample	GS Conjugates (nmol)	HNA (nmol)	Unmetabolized HNE (nmol)	Unidentified (nmoles)
HLEC	8.8 ± 2.0	6.2 ± 1.2	4.2 ± 1.2	2.9 ± 0.9
HLEC + sorbinil	9.3 ± 1.2	6.0 ± 0.9	4.4 ± 0.6	1.6 ± 0.3
HLEC + cyanamide	9.2 ± 0.3	4.5 ± 0.8*	5.1 ± 1.0	2.4 ± 0.4
Lens	16.4 ± 0.3	2.5 ± 0.5	4.3 ± 0.7	ND
Lens + sorbinil	16.0 ± 1.7	2.3 ± 1.8	3.5 ± 1.1	ND
Lens + cyanamide	15.7 ± 1.5	1.4 ± 0.6*	6.2 ± 1.9*	ND

Rat lens or HLEC (0.8×10^6 cells) were incubated with 30 nmol of HNE for 60 and 30 minutes, respectively. Approximately 5% radioactivity was retained in the rat lens and HLECs and ≃95% was present in the incubation medium. Incubation medium was filtered, filtrate equivalent to 25.0 ± 3.7 and 22.1 ± 3.0 nmol HNE from rat lens and HLECs, respectively, was applied to the HPLC column, and the HNE metabolites were separated. Fractions corresponding to the respective peaks were pooled and quantified by their radioactive counts. Recovery on HPLC of rat lens and HLEC filtrates was approximately 80%. Data are the mean ± SD of three separate experiments. ND, not detected.

* $P \leq 0.05$, significantly different (Student's *t*-test) from the control group (without inhibitors).

conjugate in rat lens is predominantly GS-HNE in the presence as well as absence of sorbinil. When HLECs were incubated with 30 nmol of [4-^{3}H] HNE, approximately 40% of the HNE added was conjugated with GSH. In the presence of sorbinil, the relative abundance of GS-HNE and GS-DHN, as estimated by ESI-MS, changed from 1:4 to 1:2 (Figs. 3E, 3F) indicating that the extruded conjugate of HLECs is predominantly in the reduced form in the absence as well as presence of sorbinil. These results further indicate that AR in the lens as well as HLECs could reduce GS-HNE to GS-DHN.

Because in most of the cells, oxidation of HNE is believed to be catalyzed by aldehyde dehydrogenase,[20–22] we investigated the effect of the aldehyde dehydrogenase inhibitor cyanamide on HNE metabolism in rat lens and HLECs. Addition of cyana-

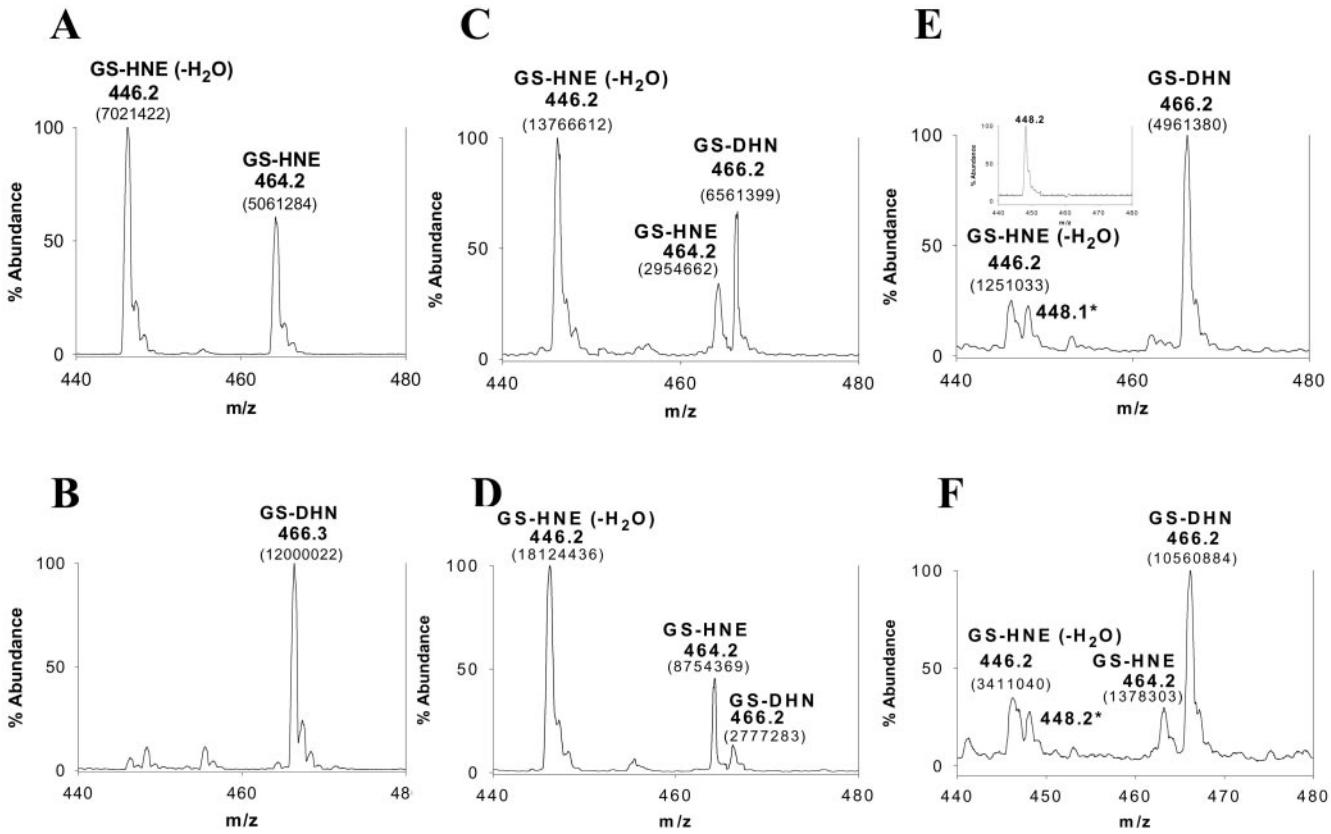

FIGURE 3. ESI-MS spectra of GS conjugates of HNE and DHN. GS conjugates of HNE (**A**) and DHN (**B**) were synthesized, purified on HPLC, and characterized by ESI-MS. In (**A**), the peak at m/z 464.2 was assigned to GS-HNE, whereas the peak at 446.2 was assigned to the daughter ion originating from dehydration of parent ion. In (**B**), the ion with an m/z of 466.2 represents GS-DHN. ESI-MS of peak I (resolved in Fig. 2B) of HPLC profile of rat lens without (**C**) and with (**D**) 50 μM sorbinil. Rat lens was preincubated with 50 μM sorbinil for 30 minutes before the addition of [4-^{3}H] HNE. The incubation medium was subjected to HPLC as in Figure 2. Pooled fractions corresponding to peak I were collected and injected into electrospray. ESI-MS of peak I (resolved in Fig. 2C) without (**E**) and with (**F**) 50 μM sorbinil. HLECs were treated the same as the rat lens. The peak at m/z 448.1 (⋆) is from the background. (**E**, *inset*) A peak at m/z 448.1 when ESI-MS was performed on peak I obtained by HPLC of HLECs incubated without HNE. The numbers in parentheses represent the arbitrary counts of the ions in the peak.

Downloaded from iovs.arvojournals.org on 06/16/2019

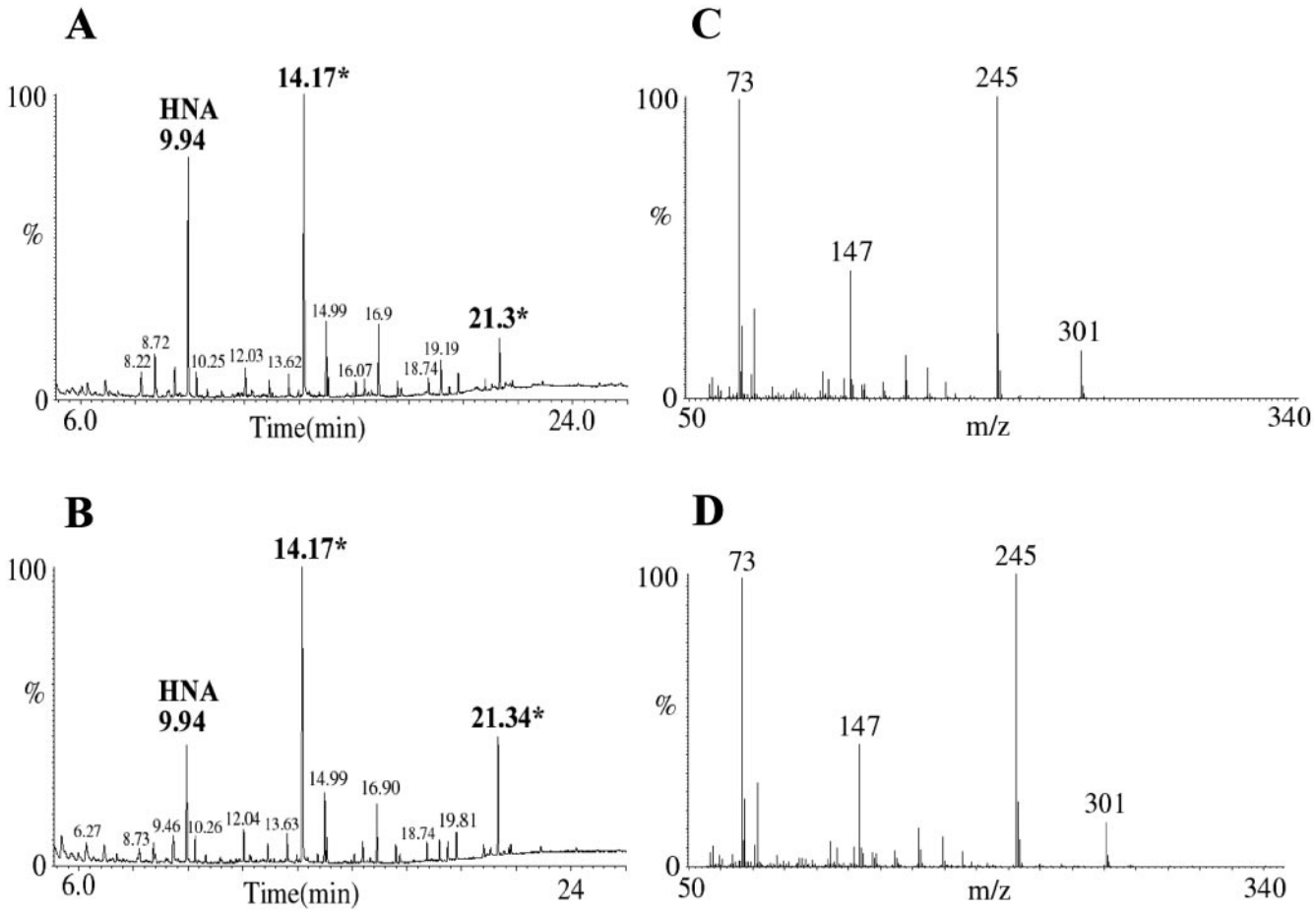

FIGURE 4. GC/CI-MS analysis of peak III obtained from HPLC separation of the incubation medium of HLECs incubated with [4-^{3}H] HNE. (**A**) GC chromatogram of synthetic HNA at τ_R 9.94 minutes. The peaks at 14.17 and 21.3 are from the background (derivatizing reagent/running solvent). (**B**) GC chromatogram of peak II in Figure 2C. The peak eluted at a τ_R of 9.94 corresponds to BSTFA-derivatized synthetic HNA. (**C**) Positive ionization mass spectrum of the peak at a τ_R of 9.94 in (**A**), showing indicated fragments at m/z 73, 83, 147 and 245. (**D**) Positive ionization mass spectrum of the peak at a τ_R of 9.94 in (**B**).

mide in the incubation medium decreased the oxidation of HNE to HNA by 44% and 27% in rat lens and HLECs, respectively (Table 1), thereby suggesting the involvement of aldehyde dehydrogenase in the oxidation of HNE in these tissues.

DISCUSSION

Because of a constant exposure to light and oxygen, the ocular lens continuously generates ROS which leads to lipid peroxidation and subsequent formation of LDAs such as HNE. Increased production of LDAs under oxidative stress necessitates their efficient metabolism to ensure the normal functioning of the lens. The results of this study show that under normal physiological conditions the rat lens and HLECs efficiently metabolized HNE through various metabolic routes. Most of the HNE added to the incubation medium rapidly entered the HLECs and lens and was metabolized and the metabolites extruded into the medium. Only a very small portion (<5%) of radioactivity was found to be retained in the lens or HLECs. The major pathway of HNE metabolism in rat lens is the conjugation of HNE with GSH. Similar to rat erythrocytes,[22] approximately, 65% and 40% of the total HNE metabolized was through GSH conjugation in rat lens and HLECs, respectively. Although HNE spontaneously conjugates with GSH, this process is facilitated by more than 300-fold[26] by one of the isozymes of glutathione *S*-transferase. This isozyme in human and bovine tissues is designated $GST_{5.8}$, in rat $GST_{8.8}$, and in mouse GST4-4.[27–29] In the lens, this isozyme is present mainly in the epithelium.[28] The GS conjugate of HNE (GS-HNE) in the tissues could be efficiently reduced to GS-DHN by AR ($K_{m\ GS\text{-}HNE}$, ~30 μM) in the presence of NADPH as described by us earlier.[30–32] As shown by the ESI-MS, the conjugate was predominantly in the reduced form in the HLECs. The GS-DHN could arise either by the AR-catalyzed reduction of GS-HNE or by conjugation of DHN with GSH. Because DHN is not electrophilic, it is unlikely that it could spontaneously react with GSH. Therefore, the most probable route of GS-DHN formation appears to be through the enzymatic reduction of GS-HNE rather than by spontaneous conjugation of DHN to GSH. The role of AR in reducing GS-HNE in rat lens and HLECs is substantiated by the observation of decreased formation of GS-DHN (reduction of GS-HNE) in the presence of the AR inhibitor sorbinil. As shown in Figures 3D and 3F, sorbinil, significantly inhibited the formation of GS-DHN (reduction of GS-HNE) in rat lens and HLECs. Thus, AR plays a significant role in the detoxification of lipid-derived aldehydes. Although, various lipid aldehydes, including HNE, are readily detoxified by conjugation with GSH and extrusion from the cells, the conjugates could still be toxic. For example, the glutathionyl conjugates of α, β unsaturated aldehydes, such as acrolein, are more toxic than their parent compounds.[33,34] One of the possible causes of the cytotoxicity of the glutathionyl conjugates of unsatur-

Downloaded from iovs.arvojournals.org on 06/16/2019

ated aldehydes could be the gradual dissociation of the electrophile–nucleophile complex. GS-HNE can spontaneously dissociate at neutral pH to form GSH and HNE.[35] Therefore, if the conjugate is not reduced, it can cause transcellular and transorgan toxicity by the release of free aldehyde. Reduction of GS-HNE to GS-DHN by AR would therefore be a major detoxification step to prevent the spread of the toxicant.

Although AR can efficiently reduce free HNE to DHN under in vitro conditions,[30–32,36] the present study shows that conversion of HNE to DHN is not a significant metabolic route for the detoxification of HNE in the rat lens or HLECs, perhaps because of the high conjugation rate of HNE to GSH, so that AR encounters mostly the GS conjugate and not the free aldehyde. Furthermore, our results show that alcohol dehydrogenase is not a major player in the detoxification of HNE. This is consistent with the finding that lens alcohol dehydrogenase displays a high K_m for HNE.[37]

The levels of GSH in HLECs (46.8 ± 2.66 nmol/mg protein) and lens (5.13 ± 0.038 mM) obtained by us are consistent with those reported earlier.[38,39] It is noteworthy that a smaller fraction of GSH present in the lens was conjugated with HNE compared with that in HLECs (Table 1). This could be due to higher specific activity of GST isozyme[28] as well as diffusion uptake of HNE by the epithelium. Our results in Figure 3 show that the effect of sorbinil on the ratio of GS-DHN to GS-HNE in the rat lens is approximately twice that in the HLECs. Because the oxidation state of AR determines the $K_{i\ sorbinil}$,[40] it is likely that the difference in the sensitivity of AR to sorbinil inhibition in the lens and HLECs could be due to the difference in the oxidative status of AR in these tissues.

In addition to conjugation, HNE in rat lens is metabolized to its corresponding acid, HNA, by aldehyde dehydrogenase. In the lens and HLECs, HNA accounted for 11% and 28%, respectively of the total metabolites. The observations that such high levels of HNA are formed and that in the presence of aldehyde dehydrogenase inhibitor, cyanamide, formation of HNA decreased by 27% and 44% in the HLECs and lens, respectively, suggest that aldehyde dehydrogenase is one of the major player in the detoxification of HNE in the lens. Our results showing higher proportion of GS-DHN and HNA in the HLECs compared with whole lens are consistent with the higher specific activity of the enzymes and cofactors in the epithelium compared to the cortex and nucleus.

In summary, we showed that HNE can be metabolized by conjugation, reduction, and oxidation. If one of the pathways is blocked, the other pathway takes over. Therefore, under normal and mild oxidizing conditions, small amounts of HNE forms partitions in the cytosol and is detoxified in the presence of GSH and other cofactors such as NADPH, NAD^+, NADP, and the HNE-metabolizing enzymes. Thus, under mild oxidative stress, the LDA-induced damage could be none or minimal. However, under severe oxidative stress, when the formation of ROS overwhelms the reduction capacity of the tissue, excessive amounts of LDAs could be formed in the membrane by oxidation of membrane lipids. Increased amounts of LDAs would then cause membrane damage by forming membrane protein adducts as well as LDA-protein cross-links, which would hamper the structural and functional integrity of the tissue, thus contributing to cataractogenesis.

Acknowledgments

The authors thank Salisha Sorbrattee for technical assistance.

References

1. Halliwell B. Reactive oxygen species in living systems: source, biochemistry and role in human disease. *Am J Med.* 1991; 91(suppl):14–22.
2. Esterbauer H, Schaur RJ, Zollner H. Chemistry and biochemistry of 4-hydroxynonenal, malondialdehyde and related aldehydes. *Free Radic Biol Med.* 1991;11:81–128.
3. Orenje WA, Wolffenbuttel BH. Lipid peroxidation and atherosclerosis in type-II diabetes. *J Lab Clin Med.* 1999;134:19–32.
4. Benedetti A, Comporti M, Esterbauer H. Identification of 4-hydroxynonenal as a cytotoxic product originating from the peroxidation of liver microsomal lipids. *Biochim Biophys Acta*. 1980; 620:281–296.
5. Esterbauer H. Lipid peroxidation products: formation, chemical properties and biological activities. In: Poli G, Cheeseman KH, Dianzani MU, Slater TF, eds. *Free Radical in Liver Injury.* Oxford, UK: IRL press; 1985;29–47.
6. Sikel W. Retinal metabolism in dark and light. In: Fuortes MGF, ed. *Handbook of Sensory Physiology*. Berlin: Springer-Verlag; 1972: 667–727.
7. Bazan NG. The metabolism of omega-3 polyunsaturated fatty acids in the eye: the possible role of docosahexaenoic acid and docosanoids in retinal physiology and ocular pathology. *Prog Clin Biol Res.* 1989;312:95–112.
8. Seth RK, Haque MS, Zelenka PS. Regulation of c-fos induction in lens epithelial cells by 12(S) HETE-dependent activation of PKC. *Invest Ophthalmol Vis Sci.* 2001;42:3239–3246.
9. Arora JK, Lysz TW, Zelenka PS. A role for 12(S)-HETE in the response of human lens epithelial cells to epidermal growth factor and insulin. *Invest Ophthalmol Vis Sci.* 1996;37:1411–1418.
10. Andley UP, Becker B, Hebert JS, Reddan JR, Morrison AR, Pentland AP. Enhanced prostaglandin synthesis after ultraviolet-B exposure modulates DNA synthesis of lens epithelial cells and lowers intraocular pressure in vivo. *Invest Ophthalmol Vis Sci.* 1996;37: 142–153.
11. Rosenfeld L, Spector A. Comparison of polyunsaturated fatty acid levels in normal and mature cataractous human lenses. *Exp Eye Res.* 1982;35:69–75.
12. Borchman D, Ozaki Y, Lamba OP, Byrdwell WC, Czarnecki MA, Yappert MC. Structural characterization of clear human lens lipid membranes by near-infrared Fourier transform Raman spectroscopy. *Curr Eye Res.* 1995;14:511–515.
13. Borchman D, Giblin FJ, Leverenz VR, et al. Impact of aging and hyperbaric oxygen in vivo on guinea pig lens lipids and nuclear light scatter. *Invest Ophthalmol Vis Sci.* 2000;4:3061–3073.
14. Yang Y, Sharma R, Cheng J-Z, et al. Protection of HLE B-3 cells against hydrogen peroxide- and naphthalene-induced lipid peroxidation and apoptosis by transfection with hGSTA1 and hGSTA2. *Invest Ophthalmol Vis Sci.* 2002;43:434–445.
15. Babizhayev MA, Deyev AI. Lens opacity induced by lipid peroxidation products as a model of cataract associated with retinal disease. *Biochim Biophys Acta* 1989;1004:124–133.
16. Zigler JS Jr, Bodaness RS, Gery I, Kinoshita JH. Effects of lipid peroxidation products on the rat lens in organ culture: a possible mechanism of cataract initiation in retinal degenerative disease. *Arch Biochem Biophys.* 1983;225:149–156.
17. Goosey JD, Tuan WM, Garcia CA. A lipid peroxidative mechanism for posterior subcapsular cataract formation in the rabbit: a possible model for cataract formation in tapetoretinal diseases. *Invest Ophthalmol Vis Sci.* 1984;25:608–612.
18. Ansari NH, Wang L, Srivastava SK. Role of lipid aldehydes in cataractogenesis: hydroxynonenal-induced cataract. *Biochem Mol Med.* 1996;58:25–30.
19. Choudhary S, Zhang W, Zhou F, et al. Cellular lipid peroxidation end products induce apoptosis in human lens epithelial cells. *Free Radic Biol Med.* 2002;32:360–469.
20. Luckey SW, Peterson DR. Metabolism of 4-hydroxynonenal by rat kupffer cells. *Arch Biochem Biophys.* 2001;389:77–83.
21. Srivastava S, Chandra A, Wang LF, et al. Metabolism of lipid peroxidation product, 4-hydroxy-trans-2-nonenal, in isolated perfused rat heart. *J Biol Chem.* 1998;273:10893–10900.
22. Srivastava S, Dixit BL, Cai J, et al. Metabolism of lipid peroxidation product, 4-hydroxynonenal (HNE) in rat erythrocytes: role of aldose reductase. *Free Radic Biol Med.* 2000;29:642–651.

Downloaded from iovs.arvojournals.org on 06/16/2019

23. Andley UP, Rhim JS, Chylack LT Jr, Fleming TP. Propagation and immortalization of human lens epithelial cells in culture. *Invest Ophthalmol Vis Sci.* 1994;35:3094–3102.
24. Ansari NH, Awasthi YC, Srivastava SK. Role of glycosylation in protein disulfide formation and cataractogenesis. *Exp Eye Res.* 1980;31:9–19.
25. Chandra A, Srivastava SK. A synthesis of 4-hydroxy-2-trans-nonenal and 4 (3H)4-hydroxy-2-trans-nonenal. *Lipids.* 1997;32:779–782.
26. Alin P, Danielson UH, Mannervik B. 4-Hydroxyalk-2-enals are substrates for glutathione transferase. *FEBS Lett.* 1985;179:267–270.
27. Singhal SS, Awasthi S, Srivastava SK, Zimniak P, Ansari NH, Awasthi YC. Novel human ocular glutathione S-transferases with high activity toward 4-hydroxynonenal. *Invest Ophthalmol Vis Sci.* 1995; 36:142–150.
28. Srivastava SK, Singhal SS, Awasthi S, Pikula S, Ansari NH, Awasthi YC. A glutathione S-transferases isozyme (bGST 5.8) involved in the metabolism of 4-hydroxy-2-*trans*-nonenal is localized in bovine lens epithelium. *Exp Eye Res.* 1996;63:329–337.
29. Laurent A, Alary J, Debrauwer L, Cravedi, JP. Analysis in the rat of 4-hydroxynonenal metabolites excreted in bile: evidence of enterohepatic circulation of these byproducts of lipid peroxidation. *Chem Res Toxicol.* 1999;12:887–894.
30. He Q, Khanna P, Srivastava S, Van Kuijk FJ, Ansari NH. Reduction of 4-hydroxynonenal and 4-hydroxyhexenal by retinal aldose reductase. *Biochem Biophys Res Commun.* 1998;247:719–722.
31. Srivastava S, Chandra A, Ansari NH, Srivastava SK, Bhatnagar A. Identification of cardiac oxidoreductase(s) involved in the metabolism of lipid peroxidation-derived aldehyde-4-hydroxynonenal. *Biochem J.* 1998;329:469–475.
32. Srivastava S, Chandra A, Bhatnagar A, Srivastava SK, Ansari NH. Lipid peroxidation product, 4-hydroxynonenal and its conjugate with GSH are excellent substrates of bovine lens aldose reductase. *Biochem Biophys Res Commun.* 1995;217:741–746.
33. Horvath JJ, Witmer CM, Witz G. Nephrotoxicity of the 1:1 acrolein-glutathione adduct in the rat. *Toxicol Appl Pharm.* 1992;117:200–207.
34. Adams JD Jr, Klaidman LK. Acrolein-induced oxygen radical formation. *Free Radic Biol Med.* 1993;15:187–193.
35. Esterbauer H, Zollner H, Scholz N. Reaction of glutathione with conjugated carbonyls. *Z Naturforsch.* 1975;30:466–473.
36. Vander Jagt DL, Kolb NS, Vander Jagt TJ, et al. Substrate specificity of human aldose reductase: identification of 4-hydroxynonenal as an endogenous substrate. *Biochim Biophys Acta.* 1995;1249:117–126.
37. Holmes RS, Vanderber JL. Ocular NAD-dependent alcohol dehydrogenase and aldehyde dehydrogenase in the baboon. *Exp Eye Res.* 1986;43:383–396.
38. Kannan R, Ouyang B, Wawrousek E, Kaplowitz N, Andley UP. Regulation of GSH in alphaA-expressing human lens epithelial cell lines and in alphaA knockout mouse lenses. *Invest Ophthalmol Vis Sci.* 2001;42:409–416.
39. Srivastavs SK, Ansari NH. Prevention of sugar-induced cataractogenesis in rats by butylated hydroxytoluene. *Diabetes* 1988;38: 1505–1508.
40. Srivastava SK, Hair GA, Das B. Activated and unactivated forms of human erythrocyte aldose reductase. *Proc Natl Acad Sci USA.* 1985;82:7222–7226.

Downloaded from iovs.arvojournals.org on 06/16/2019